

## Regulated iron corrosion towards fabricating large-area self-supporting electrodes for efficient oxygen evolution reaction

Xupo Liu<sup>a, b, †</sup>, Xuyun Guo<sup>c, †</sup>, Mingxing Gong<sup>a</sup>, Tonghui Zhao<sup>a</sup>, Jian Zhang<sup>a</sup>, Ye Zhu<sup>c</sup>, Deli Wang<sup>a,\*</sup>

<sup>a</sup>*Key Laboratory of Material Chemistry for Energy Conversion and Storage, Ministry of Education, Hubei Key Laboratory of Material Chemistry and Service Failure, School of Chemistry and Chemical Engineering, Huazhong University of Science and Technology, Wuhan, 430074, P.R. China.*

<sup>b</sup>*School of Materials Science and Engineering, Henan Normal University, Xinxiang, 453007, P. R. China.*

<sup>c</sup>*Department of Applied Physics, The Hong Kong Polytechnic University, Hung Hom, Hong Kong, P. R. China.*

<sup>†</sup>Xupo Liu and Xuyun Guo contributed equally to the work.

E-mail: wangdl81125@hust.edu.cn.

**Table S1** Comparison of the standard potentials for different electrode pairs.<sup>a</sup>

Electrode pairs	Potential values / V	Electrode pairs	Potential values / V
Ni <sup>2+</sup> /Ni	-0.257	Zn <sup>2+</sup> /Zn	-0.762
Fe <sup>2+</sup> /Fe	-0.447	Co <sup>2+</sup> /Co	-0.280
Fe <sup>3+</sup> /Fe	-0.037	Fe <sup>3+</sup> /Fe <sup>2+</sup>	+0.771
O <sub>2</sub> /OH <sup>-</sup>	+0.401	Fe(OH) <sub>3</sub> /Fe(OH) <sub>2</sub>	-0.560

<sup>a</sup> These values are all cited from the book: D. R. Lide, CRC Handbook of Chemistry and Physics (84th edn), CRC Press, Boca Raton, Florida, USA 2004.

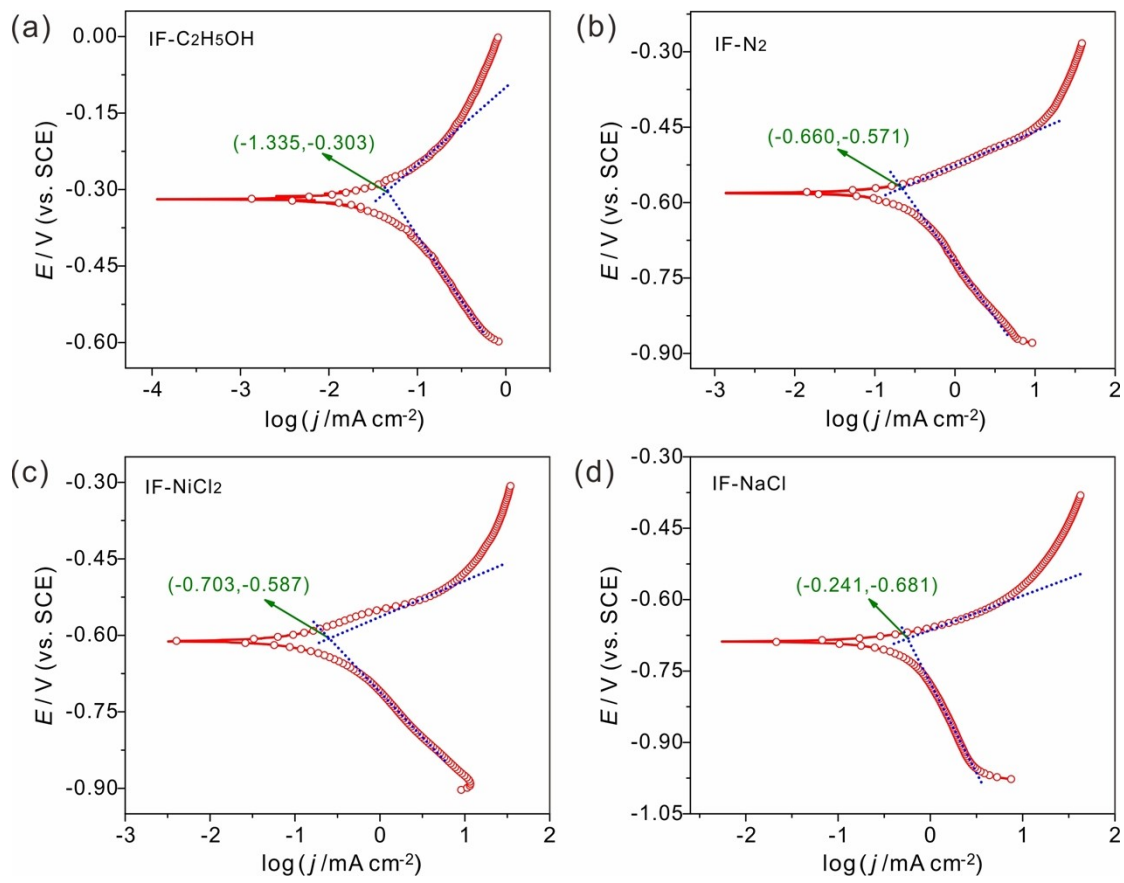


**Fig. S1.** The fitted corrosion polarization curves for achieving corrosion potentials and current densities: (a) IF-C<sub>2</sub>H<sub>5</sub>OH, (b) IF-N<sub>2</sub>, (c) IF-NiCl<sub>2</sub> and (d) IF-NaCl.

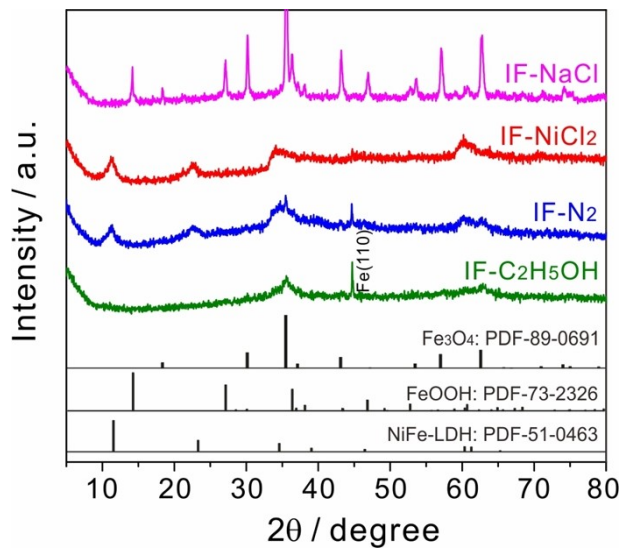


**Fig. S2.** XRD patterns of corrosion layers for IF-C<sub>2</sub>H<sub>5</sub>OH, IF-N<sub>2</sub>, IF-NiCl<sub>2</sub> and IF-NaCl.

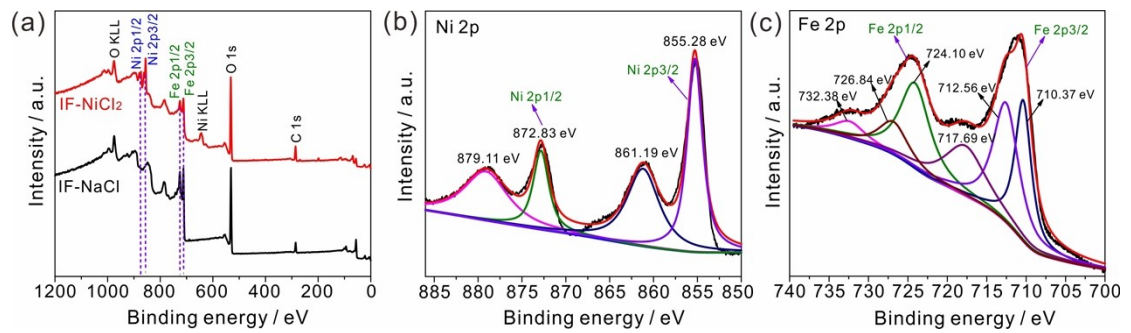


**Fig. S3.** (a) Comparison of XPS spectra for IF-NaCl and IF-NiCl<sub>2</sub>, (b) Ni 2p spectrum and (c) Fe 2p spectrum of IF-NiCl<sub>2</sub>.

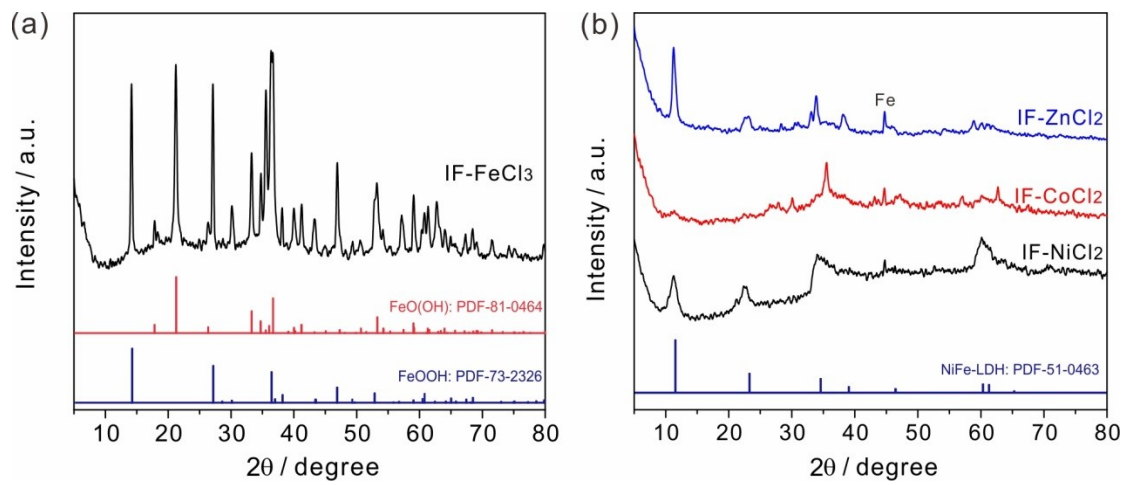


**Fig. S4.** (a) XRD pattern of IF-FeCl<sub>3</sub>, (b) XRD patterns of IF-NiCl<sub>2</sub>, IF-CoCl<sub>2</sub> and IF-ZnCl<sub>2</sub>.

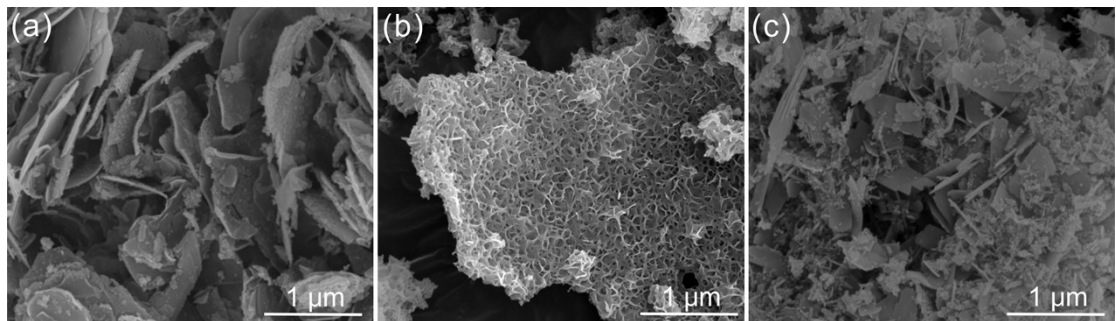


**Fig. S5.** SEM images: (a) IF-ZnCl<sub>2</sub>, (b) IF-CoCl<sub>2</sub> and (c) IF-FeCl<sub>3</sub>.

The different micromorphologies of corrosion layers are presented in above images. The corrosion degree follows the order: ZnCl<sub>2</sub> < NiCl<sub>2</sub> < CoCl<sub>2</sub> < FeCl<sub>3</sub>. The metal ions with different electrode potentials bring forth the diverse corrosion process. Actually, the oxygen corrosion happens in all the chloride solutions, while there are extra reactions occurring for iron corrosion in NiCl<sub>2</sub>, CoCl<sub>2</sub> and FeCl<sub>3</sub> solutions. The suitable electrode potentials, close to those of Ni<sup>2+</sup>/Ni and Co<sup>2+</sup>/Co, are necessary for achieving the uniform corrosion layers, which is responsible for achieving high electrochemical activity and durability. The too high or too low standard electrode potential for Fe<sup>3+</sup>/Fe<sup>2+</sup> or Zn<sup>2+</sup>/Zn results in the serious or weak corrosion behaviors, leading to uneven growth of corrosion layers.

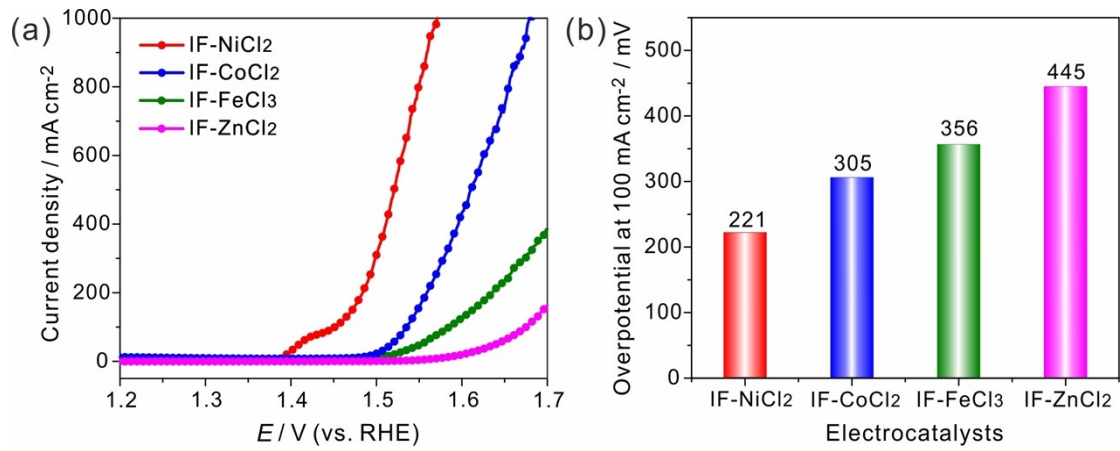


**Fig. S6.** (a) Polarization curves of IF-NiCl<sub>2</sub>, IF-CoCl<sub>2</sub>, IF-FeCl<sub>3</sub> and IF-ZnCl<sub>2</sub>; (b) comparison of the overpotentials at the current density of 100  $\text{mA cm}^{-2}$ .

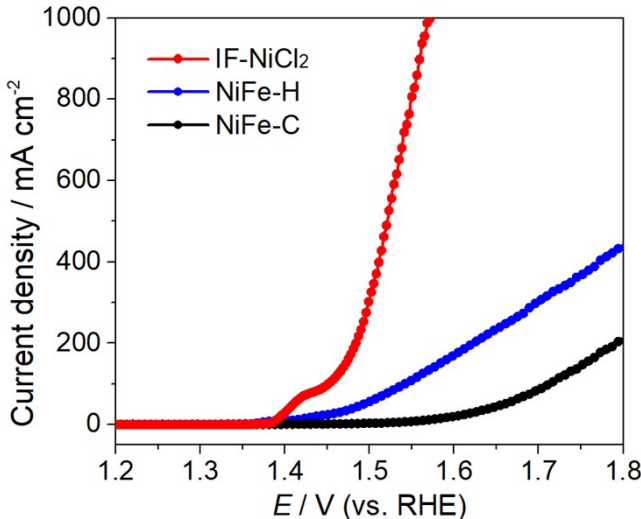


**Fig. S7.** Polarization curves of IF-NiCl<sub>2</sub>, NiFe-H and NiFe-C.

Two reference samples were synthesized by the hydrothermal and co-precipitation methods, respectively. The preparation process was as follows. (i) Hydrothermal synthesis. The cleaned iron foam was immersed in 30 mL of 100 mM NiCl<sub>2</sub> solution in a 50 mL Teflon-lined autoclave, which was kept at 150 °C for 6 h. After cooling down, the electrode was washed with deionized water and ethanol for several times, and then dried under vacuum at 60 °C overnight. The obtained catalyst was donated as NiFe-H. (ii) Co-precipitation preparation. Firstly, 3 mmol NiCl<sub>2</sub> and 1 mmol FeCl<sub>3</sub> were dissolved in 30 mL deionized water. Then, 20 mL of 450 mM NaOH was dropwise added in the above solution. After stirring for 30 min, the precipitates were obtained by centrifugation and washing with water. Through drying at 60 °C, the final products were achieved, which was donated as NiFe-C. The OER performance of these samples was determined. It can be seen that the IF-NiCl<sub>2</sub> sample only needs the small overpotential of 221 mV to achieve the current density of 100 mA cm<sup>-2</sup>, much lower than those of NiFe-H (312 mV) and NiFe-C (484 mV). The better OER activity of IF-NiCl<sub>2</sub> confirms the superiority of corrosion engineering.

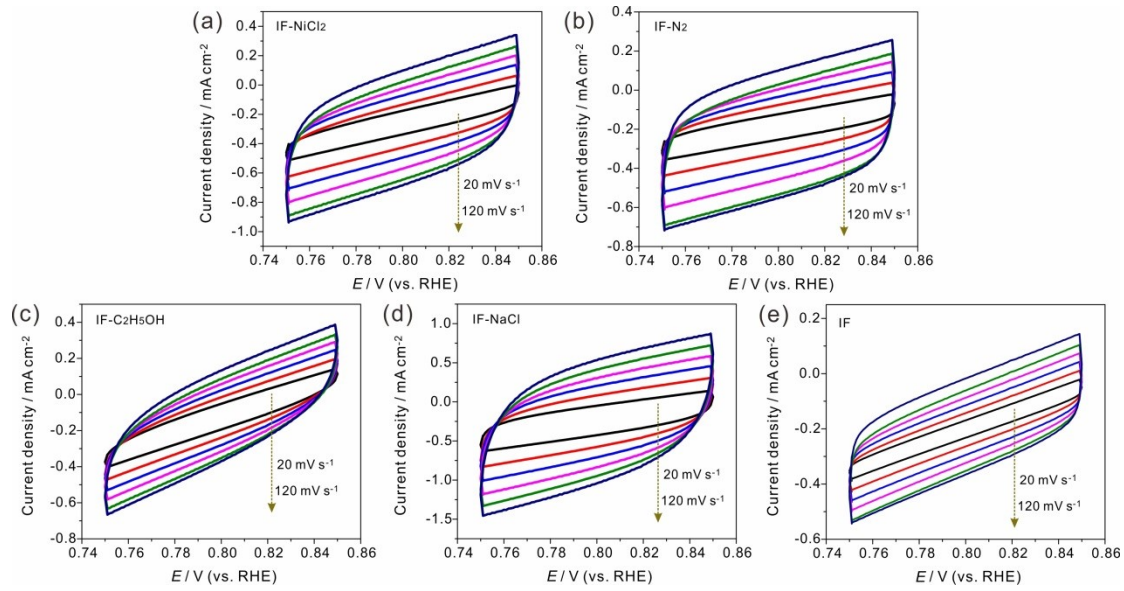


**Fig. S8.** CV curves in the potential range of 0.75–0.85 V at the different scan rates: (a) IF-NiCl<sub>2</sub>, (b) IF-N<sub>2</sub>, (c) IF-C<sub>2</sub>H<sub>5</sub>OH, (d) IF-NaCl and (e) pristine IF.

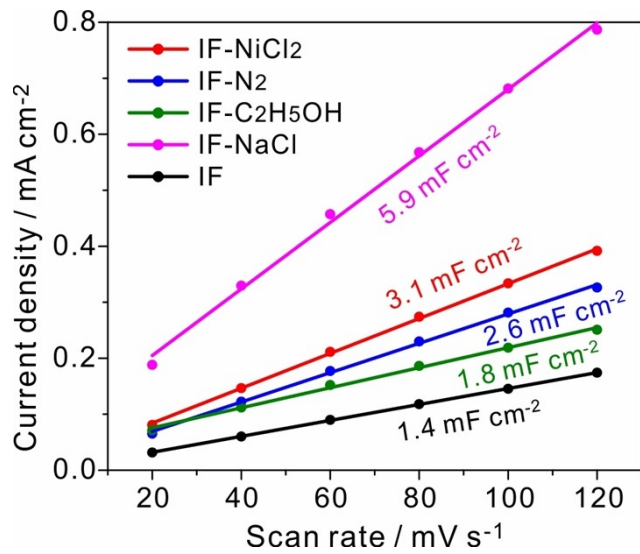


**Fig. S9.** Linear fitting of capacitive current density at 0.8 V depending on scan rates.

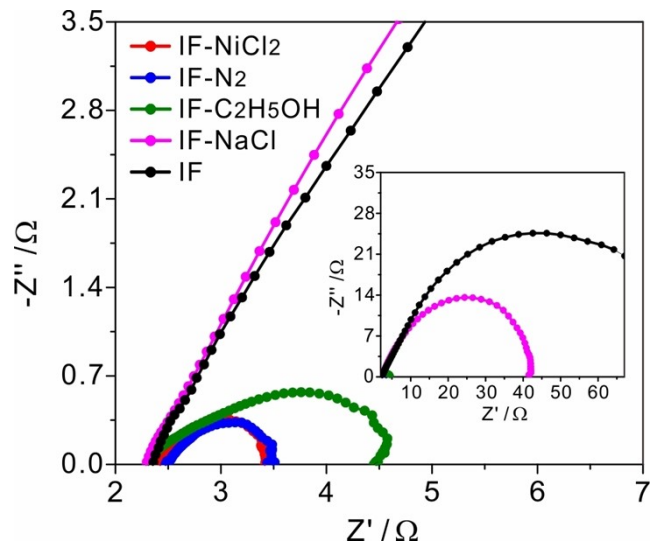


**Fig. S10.** Nyquist curves of IF-NiCl<sub>2</sub>, IF-N<sub>2</sub>, IF-C<sub>2</sub>H<sub>5</sub>OH, IF-NaCl and IF.

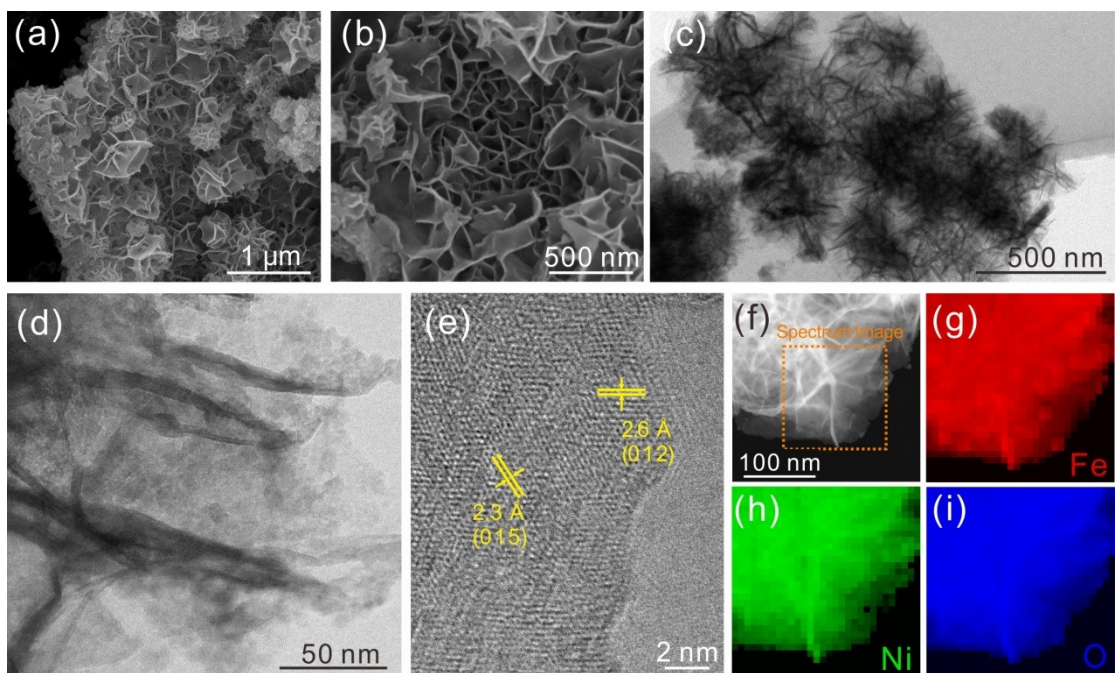


**Fig. S11.** Characterization of IF-NiCl<sub>2</sub> after the stability test: (a-b) SEM images, (c-d) TEM images, (e) HRTEM image, (f-i) HAADF-STEM image and corresponding EELS elemental maps.

**Table S2** Comparison of OER activity and stability for the recently published electrocatalysts in 1.0 M KOH electrolyte.

Sample	Overpotentials at 100 mA cm <sup>-2</sup> (mV)	Tafel slopes (mV dec <sup>-1</sup> )	Stability test	References
IF-NiCl <sub>2</sub>	221	18.3	500 mA cm <sup>-2</sup> for 100 h	This work
NiFe-OH-F-SR	228	22.6	50 mA cm <sup>-2</sup> for 165 h	1
Ni-Fe-OH@Ni <sub>3</sub> S <sub>2</sub> /NF	240	93	500 mA cm <sup>-2</sup> for 50 h	2
a-NiFe NS/IF	240	31.8	100 mA cm <sup>-2</sup> for 48 h	3
Cr <sub>1</sub> /FeNi-LDH-SS	242	32.5	10-20 mA cm <sup>-2</sup> for 15 h	4
FNS/NiSe	242	61.3	100 mA cm <sup>-2</sup> for 12 h	5
NiFe-NFF	253	38.9	10-20 mA cm <sup>-2</sup> for 15 h	6
S-NiFe <sub>2</sub> O <sub>4</sub> /Ni <sub>3</sub> Fe/NW	260	35	100 mA cm <sup>-2</sup> for 110 h	7
Ir/Ni(OH) <sub>2</sub>	270	41	20 mA cm <sup>-2</sup> for 6 h	8
NiCo <sub>2</sub> S <sub>4</sub>	277	38.7	10 mA cm <sup>-2</sup> for 20 h	9
S-(Ni,Fe)OOH	281	48.9	100 mA cm <sup>-2</sup> for 100 h	10
CuCo <sub>2</sub> S <sub>4</sub> /PANI/NF	291	68	1.83 V for 40 h	11
Ni <sub>5</sub> Co <sub>3</sub> Mo-OH	304	56.4	100 mA cm <sup>-2</sup> for 100 h	12
316SS CCE-10h	320	---	400 mA cm <sup>-2</sup> for 20 h	13
CoSe <sub>2</sub> -Ni <sub>3</sub> Se <sub>2</sub> /NF	344	68.8	20 mA cm <sup>-2</sup> for 10 h	14
2D Co <sub>3</sub> O <sub>4</sub>	380	62	1.55 V for 12 h	15
Ni-Mo-S	390	103	15 mA cm <sup>-2</sup> for 12 h	16
NCP/G NSs	400	65.9	50 mA cm <sup>-2</sup> for 20 h	17
C MS Ni(OH) <sub>2</sub>	440	66	10 mA cm <sup>-2</sup> for 10 h	18

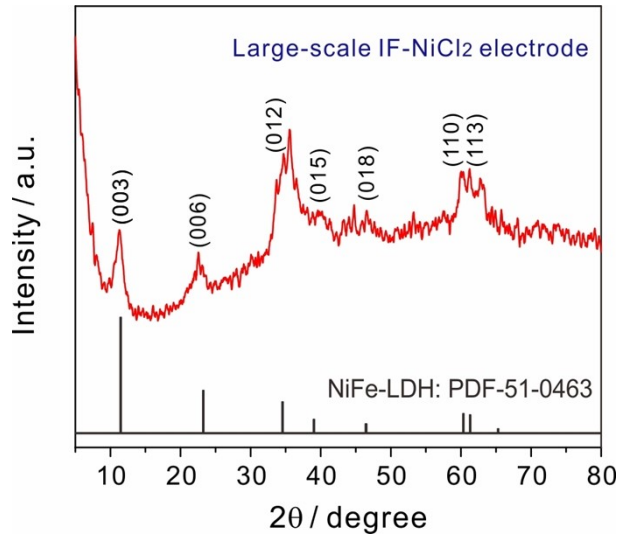


**Fig. S12.** XRD pattern of the large-scale IF-NiCl<sub>2</sub> electrode

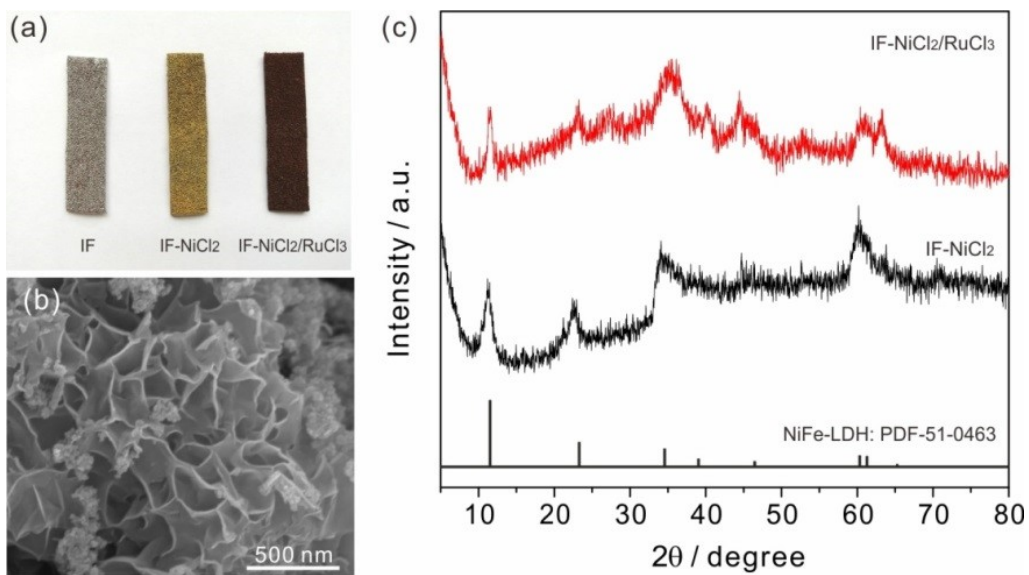


**Fig. S13.** (a) Photographs of the pristine IF, IF-NiCl<sub>2</sub> and IF-NiCl<sub>2</sub>/RuCl<sub>3</sub>; (b) SEM image of IF-NiCl<sub>2</sub>/RuCl<sub>3</sub>; (c) XRD patterns of IF-NiCl<sub>2</sub> and IF-NiCl<sub>2</sub>/RuCl<sub>3</sub>.

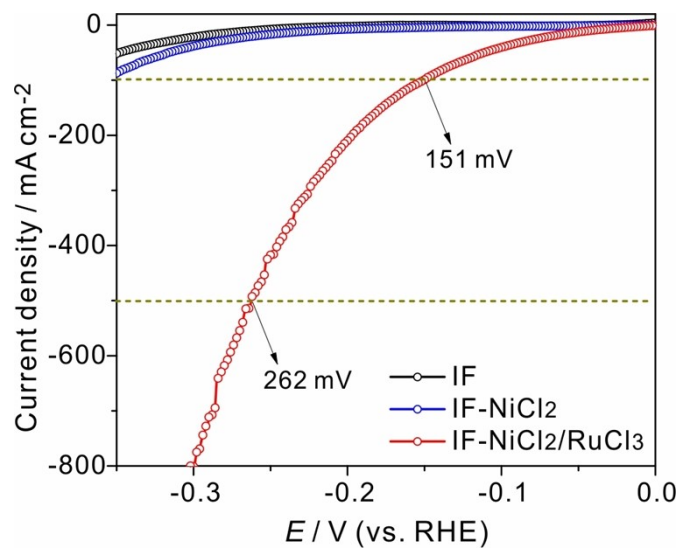
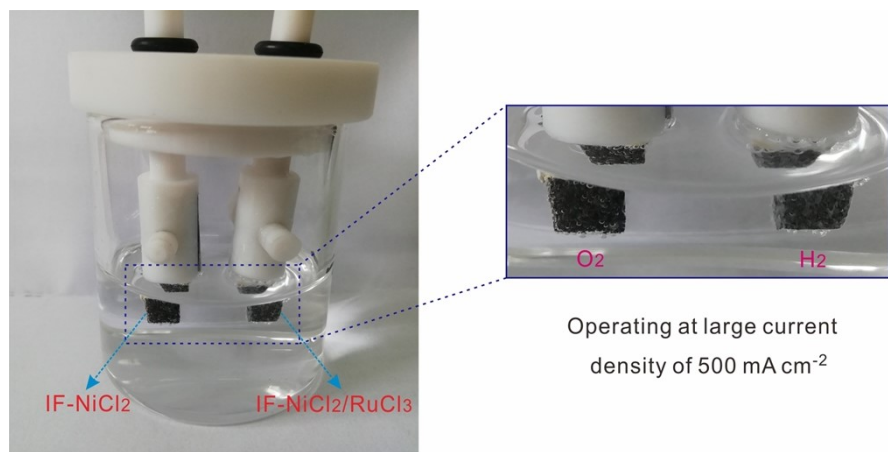


**Fig. S14.** HER polarization curves of IF, IF-NiCl<sub>2</sub> and IF-NiCl<sub>2</sub>/RuCl<sub>3</sub>.



Operating at large current density of  $500 \text{ mA cm}^{-2}$

**Fig. S15.** The assembled water-splitting cell by IF-NiCl<sub>2</sub> and IF-NiCl<sub>2</sub>/RuCl<sub>3</sub> operates at the large current density of  $500 \text{ mA cm}^{-2}$ .

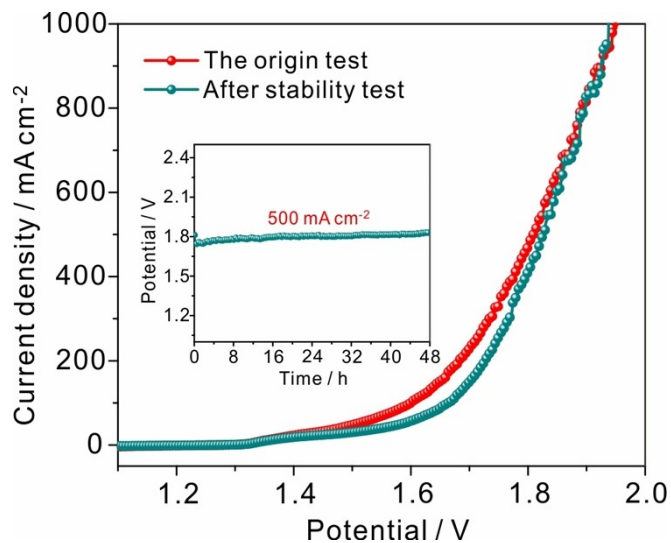


**Fig. S16.** Comparison of polarization curves before and after stability determination (inset: chronopotentiometric curve at  $500 \text{ mA cm}^{-2}$  for 48 h).

**Table S3** Comparison of overall water-splitting performances of the recently published electrocatalysts in 1.0 M KOH electrolyte.

OER electrode	HER electrode	Voltage/Current density (mV/mA cm <sup>-2</sup> )	Stability determination	References
IF-NiCl <sub>2</sub>	IF-NiCl <sub>2</sub> /RuCl <sub>3</sub>	1.60/100, 1.81/500	500 mA cm <sup>-2</sup> for 48 h	This work
NiFe-LDH	PB <sub>0.94</sub> C-DSPH	1.93/500	500 mA cm <sup>-2</sup> for 10 h	19
Ni <sub>0.46</sub> Co <sub>0.54</sub> -400	Ni <sub>0.46</sub> Co <sub>0.54</sub> -400	1.68/500	500 mA cm <sup>-2</sup> for 30 h	20
NiFe-LDH/NF	RFNOH-10	1.60/100, 1.69/500	500 mA cm <sup>-2</sup> for 20 h	21
(Ni, Fe)OOH	MoNi <sub>4</sub>	1.586/500	500 mA cm <sup>-2</sup> for 35 h	22
0.14M Fe/A-NF	0.14M Fe/A-NF	1.99/500	500 mA cm <sup>-2</sup> for 24 h	23
NiFe(OH) <sub>x</sub> /FeS/IF	MoNi <sub>4</sub> /MoO <sub>2</sub> /NF	1.95/300	300 mA cm <sup>-2</sup> for 70 h	24
S-CoO <sub>x</sub>	S-CoO <sub>x</sub>	1.85/100	100 mA cm <sup>-2</sup> for 29 h	25
FF-Na <sub>500</sub> Ni <sub>500</sub>	FF-Na <sub>500</sub> Ni <sub>500</sub>	1.71/100	100 mA cm <sup>-2</sup> for 168 h	26
a-CoMoP <sub>x</sub> /CF	a-CoMoP <sub>x</sub> /CF	1.703/100	100 mA cm <sup>-2</sup> for 100 h	27
Ni <sub>5</sub> Co <sub>3</sub> Mo-OH	Ni <sub>5</sub> Co <sub>3</sub> Mo-OH	1.43/10, 1.60/100	100 mA cm <sup>-2</sup> for 100 h	12
Ni <sub>30</sub> Fe	NiCu	1.71/400	20-100 mA cm <sup>-2</sup> for 12 h	28
Ru-MnFeP/NF	Ru-MnFeP/NF	1.47/10	20 mA cm <sup>-2</sup> for 50 h	29
δ-FeOOH/Ni <sub>3</sub> S <sub>2</sub> /NF	δ-FeOOH/Ni <sub>3</sub> S <sub>2</sub> /NF	1.525/10	20 mA cm <sup>-2</sup> for 48 h	30
(Fe <sub>0.1</sub> Ni <sub>0.9</sub> ) <sub>2</sub> P(O)/NF	(Fe <sub>0.1</sub> Ni <sub>0.9</sub> ) <sub>2</sub> P(O)/NF	1.50/10, 1.70/100	20 mA cm <sup>-2</sup> for 40 h	31
VOOH-3Fe	VOOH-3Fe	1.53/10	10 mA cm <sup>-2</sup> for 48 h	32

## References

- 1 B. Zhang, K. Jiang, H. Wang and S. Hu, *Nano Lett.*, 2018, **19**, 530-537.
- 2 X. Zou, Y. Liu, G.-D. Li, Y. Wu, D.-P. Liu, W. Li, H.-W. Li, D. Wang, Y. Zhang and X. Zou, *Adv. Mater.*, 2017, **29**, 1700404.
- 3 X. Yang, Q.-Q. Chen, C.-J. Wang, C.-C. Hou and Y. Chen, *J. Energy Chem.*, 2019, **35**, 197-203.
- 4 X. Xie, C. Cao, W. Wei, S. Zhou, X. T. Wu and Q. L. Zhu, *Nanoscale*, 2020, **12**, 5817-5823.
- 5 S. Ma, H. Yuan, L. Cai, X. Wang, H. Long, Y. Chai and Y. H. Tsang, *Mater. Today Chem.*, 2018, **9**, 133-139.
- 6 C. Cao, D. D. Ma, Q. Xu, X. T. Wu and Q. L. Zhu, *Adv. Funct. Mater.*, 2018, **29**, 1807418.
- 7 M. Y. Gao, J. R. Zeng, Q. B. Zhang, C. Yang, X. T. Li, Y. X. Hua and C. Y. Xu, *J. Mater. Chem. A*, 2018, **6**, 1551-1560.
- 8 G. Zhao, P. Li, N. Cheng, S. X. Dou and W. Sun, *Adv. Mater.*, 2020, **32**, 2000872.
- 9 S. Chang, X. Huang, C. Y. Aaron Ong, L. Zhao, L. Li, X. Wang and J. Ding, *J. Mater. Chem. A*, 2019, **7**, 18338-18347.
- 10 L. Yu, L. Wu, B. McElhenny, S. Song, D. Luo, F. Zhang, Y. Yu, S. Chen and Z. Ren, *Energy Environ. Sci.*, 2020, DOI: 10.1039/d0ee00921k.
- 11 W. Sun, W. Wei, N. Chen, L. Chen, Y. Xu, C. J. Oluigbo, Z. Jiang, Z. Yan and J. Xie, *Nanoscale*, 2019, **11**, 12326-12336.
- 12 S. Hao, L. Chen, C. Yu, B. Yang, Z. Li, Y. Hou, L. Lei and X. Zhang, *ACS Energy Lett.*, 2019, **4**, 952-959.
- 13 N. Todoroki and T. Wadayama, *ACS Appl. Mater. Interfaces*, 2019, **11**, 44161-44169.
- 14 Y. Han, H. Li, M. Zhang, Y. Fu, Y. Liu, Y. Yang, J. Xu, Y. Geng and L. Wang, *Appl. Surf. Sci.*, 2019, **495**, 143606.
- 15 Y. Kang, H. Xie, D. Liu, M. Gao, P. K. Chu, S. Ramakrishna and X. F. Yu, *Chem. Commun.*, 2019, **55**, 11406-11409.
- 16 Z. Ma, H. Meng, M. Wang, B. Tang, J. Li and X. Wang, *ChemElectroChem*, 2018, **5**, 335-342.
- 17 J. Tian, J. Chen, J. Liu, Q. Tian and P. Chen, *Nano Energy*, 2018, **48**, 284-291.
- 18 V. Maruthapandian, A. Muthurasu, A. Dekshinamoorthi, R. Aswathy, S. Vijayaraghavan, S. Muralidharan and V. Saraswathy, *ChemElectroChem*, 2019, **6**, 4391-4401.

- 19 Y. Liu, Y. Dou, S. Li, T. Xia, Y. Xie, Y. Wang, W. Zhang, J. Wang, L. Huo and H. Zhao, *Small Methods*, 2020, **5**, 2000701.
- 20 K. Zhou, Q. Zhang, J. Liu, H. Wang and Y. Zhang, *J. Mater. Chem. A*, 2020, **8**, 4524-4532.
- 21 X. Xiao, X. Wang, X. Jiang, S. Song, D. Huang, L. Yu, Y. Zhang, S. Chen, M. Wang, Y. Shen and Z. Ren, *Small Methods*, 2020, **4**, 1900796.
- 22 H. Zhou, F. Yu, Q. Zhu, J. Sun, F. Qin, L. Yu, J. Bao, Y. Yu, S. Chen and Z. Ren, *Energy Environ. Sci.*, 2018, **11**, 2858-2864.
- 23 X.-F. Chuah, C.-T. Hsieh, C.-L. Huang, D. Senthil Raja, H.-W. Lin and S.-Y. Lu, *ACS Applied Energy Materials*, 2018, **2**, 743-753.
- 24 S. Niu, W. J. Jiang, T. Tang, L. P. Yuan, H. Luo and J. S. Hu, *Adv. Funct. Mater.*, 2019, **29**, 1902180.
- 25 X. Yu, Z. Yu, X. Zhang, P. Li, B. Sun, X. Gao, K. Yan, H. Liu, Y. Duan, M. Gao, G. Wang and S. Yu, *Nano Energy*, 2020, **71**, 104652.
- 26 X. Liu, M. Gong, D. Xiao, S. Deng, J. Liang, T. Zhao, Y. Lu, T. Shen, J. Zhang and D. Wang, *Small*, 2020, **16**, 2000663.
- 27 H. Huang, A. Cho, S. Kim, H. Jun, A. Lee, J. W. Han and J. Lee, *Adv. Funct. Mater.*, 2020, **30**, 2003889.
- 28 X. Teng, J. Wang, L. Ji, Y. Liu, C. Zhang and Z. Chen, *ACS Sustainable Chem. Eng.*, 2019, **7**, 5412-5419.
- 29 D. Chen, Z. Pu, R. Lu, P. Ji, P. Wang, J. Zhu, C. Lin, H. W. Li, X. Zhou, Z. Hu, F. Xia, J. Wu and S. Mu, *Adv. Funct. Mater.*, 2020, **10**, 2000814.
- 30 X. Ji, C. Cheng, Z. Zang, L. Li, X. Li, Y. Cheng, X. Yang, X. Yu, Z. Lu, X. Zhang and H. Liu, *J. Mater. Chem. A*, 2020, **8**, 21199-21207.
- 31 C. Lin, D. Wang, H. Jin, P. Wang, D. Chen, B. Liu and S. Mu, *J. Mater. Chem. A*, 2020, **8**, 4570-4578.
- 32 J. Zhang, R. Cui, C. Gao, L. Bian, Y. Pu, X. Zhu, X. Li and W. Huang, *Small*, 2019, **15**, 1904688.